

PAPER • OPEN ACCESS

Research on counter-roller spinning force based on finite element simulation and experiment

To cite this article: Yaming Guo *et al* 2019 *IOP Conf. Ser.: Mater. Sci. Eng.* **563** 042069

View the [article online](#) for updates and enhancements.



IOP | ebooks™

Bringing you innovative digital publishing with leading voices to create your essential collection of books in STEM research.

Start exploring the collection - download the first chapter of every title for free.

Research on counter-roller spinning force based on finite element simulation and experiment

Yaming Guo^{1,2,3}, Mingzhe Li^{1,2*}, Tao Huang³, Dali Wang³, Hongwei Zheng^{1,3}, Wei Luo^{1,3}, Yinan Li³, Wulin Gao³, Xing Zhao³

¹College of Materials Science and Engineering, Jilin University, Changchun, Jilin, 130025, China

²Dieless Forming Technology Center, Roll Forging Institute, Jilin University, Changchun, Jilin, 130025, China

³Changchun Equipment & Technology Research Institute, Changchun, Jilin, 130012, China

*Corresponding author's e-mail: limz@jlu.edu.cn

Abstract. Counter-roller spinning is an effective method for forming large metal cylindrical parts. In this paper, the radial, axial and tangential counter-roller spinning forces were analyzed. The simulation analysis model was established and the counter-roller spinning was simulated based on the commercial FEA software, SIMUFACT-FORMING. The influence of different thinning ratio, feed rate and forming angle of roller on spinning force was analyzed. It can be seen that the deviation between the simulation average radial spinning force and the experiment average radial spinning force was less than 12%, and that of the axial spinning force is less than 10.5%, which can effectively guide the spinning process test.

1. Introduction

Counter-roller spinning is an effective method for forming large metal cylindrical parts, which is developed on the basis of traditional mandrel spinning [1]. It uses the inner spinning rollers instead of the traditional mandrel. When the blank is deformed, it is very easy to lose its stability without the support of the internal mandrel. Therefore, the balance of spinning force directly affects the success of forming [2]. The spinning force is mainly related to thinning ratio, feed rate and contact area between the roller and blank. Generally, three or four pairs are selected in counter-roller spinning process[3].

2. Establishment of FEA model

This paper adopts backward forming, and the FE simulation model of counter-roller spinning is established by SIMUFACT-FORMING software (as shown in Figure 1). The blank is fixed by the snap ring and rotate synchronously with the snap ring in the model. The rollers feed along the axial direction. When the rollers touch the blank, they rotate along their own axis due to the effect of friction [4]. The rollers, mandrel and snap ring are defined as pure rigid body and the blank as variable body. The blank was meshed with eight-node hexahedral element with 10 layers along the thickness direction. The Coulomb friction coefficient was determined as 0.1.

The blank material is 30CrMnSiA, with tensile strength $\sigma_b=685\text{MPa}$, yield strength $\sigma_s=370\text{MPa}$, elongation $\delta=19.1\%$, and section shrinkage $\psi=55.9\%$. The relation between the true stress and true strain is $\sigma=1152.841\varepsilon^{0.217}$. Mechanical properties of the blank were obtained by axial stretching at



room temperature [5]. The main processing parameters are as follows: inner diameter of tubular blank $\phi=1970\text{mm}$, thickness of tubular blank $t_0=26\text{ mm}$; the geometric dimensions of the inner and outer rollers are the same with roundness radius $r_\rho=6\text{ mm}$ and diameter $D_\rho=260\text{mm}$; rotational speed of mandrel $n=15\text{r/min}$; the axial distance between each pair of roller $l=0\text{ mm}$; thinning ratio of tubular blank $\Psi_t = 20,30,40,50,$ and 76% ; forming angle of roller $\alpha_\rho= 20^\circ, 25^\circ,$ and 30° ; feed rates of roller $f=1.0, 1.5,$ and 2.0mm/r . The reduction amount of the inner and outer rollers was determined based on the following principle: the contact area between the inner roller and blank is equal to that between the outer roller and blank. The outer spinning rollers are referred to as OR, and the inner spinning rollers are referred to as IR.

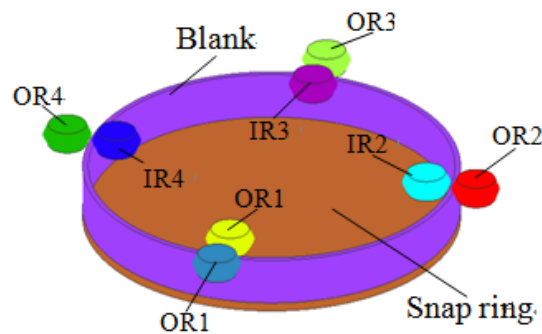


Figure 1 FEA model

3. Simulation results and analysis

3.1. Spinning force of OR and IR

Figure 2, Figure 3 and Figure 4 respectively show the axial, radial and tangential spinning force under these process parameters, which are as follows: thinning ratio $\Psi_t = 20\%$, feed rate $f=1.0\text{ mm/r}$, forming angle of roller $\alpha_\rho=25^\circ$. The axial spinning force curves of the four outer rollers basically coincide, and the radial and tangential forces of that also basically coincide. The spinning force of the inner rollers also has the same rule. Therefore, only the spinning force of the pair of OR3 and IR3 rollers were analysed, since the forces of the other pairs of rollers were similar.

The radial spinning forces of the inner and outer rollers were in opposite directions. The axial and tangential forces of that were in same directions, respectively. In the initial spinning stage, the axial, radial and tangential spinning forces of the outer rollers are correspondingly higher than those of the inner rollers. In the stable stage of deformation, the difference of spinning force between the inner roller and outer roller decreases.

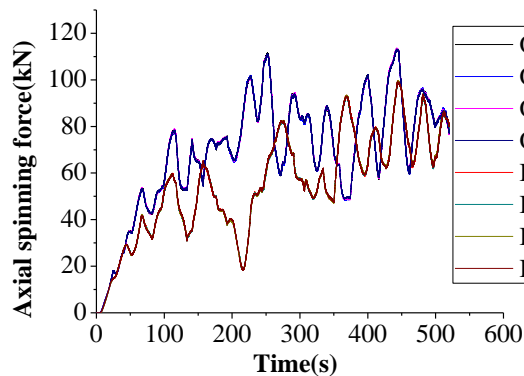


Figure 2 Axial Spinning force

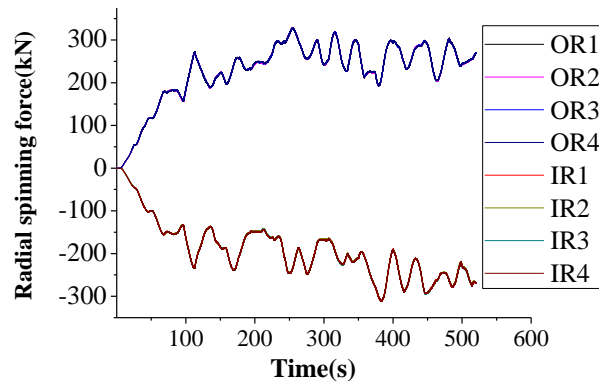


Figure 3 Radial Spinning force

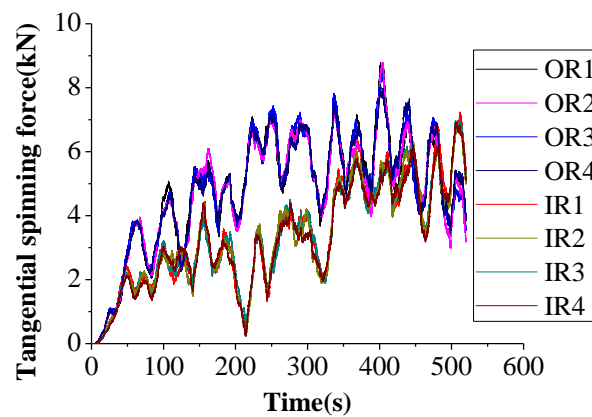


Figure 4 Tangential Spinning force

3.2. Effect of different thinning ratios on spinning force

The radial, axial and tangential spinning force of OR3 respectively present a gradually increasing trend with the increase of the thinning ratio, and that of IR3 respectively present the same trend, as shown in Figure 5~Figure 9. Therefore, only the spinning force of OR3 roller was analysed in the following.

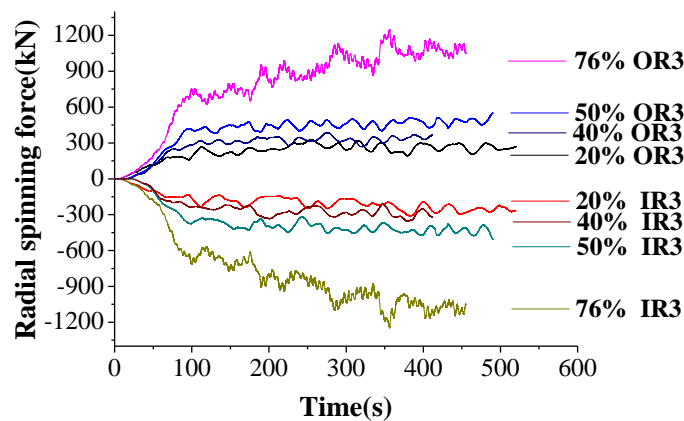


Figure 5 Radial spinning force of OR3 and IR3

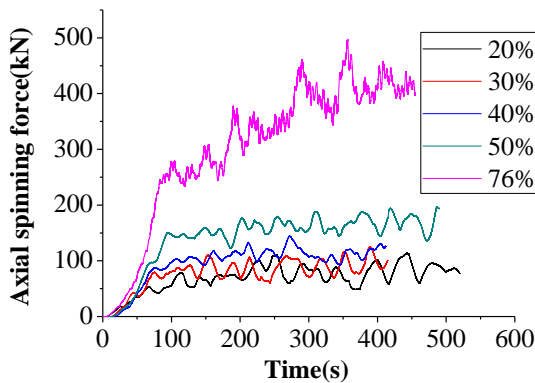


Figure 6 Axial spinning force of OR3

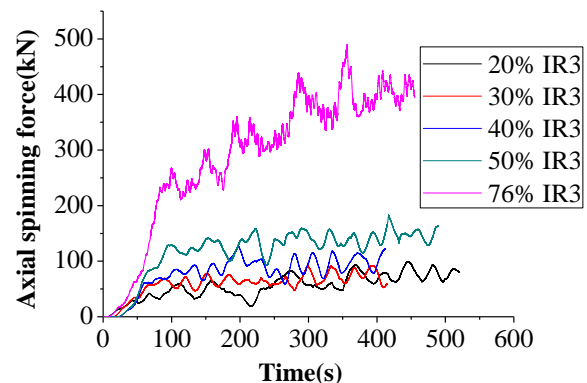


Figure 7 Axial spinning force of IR3

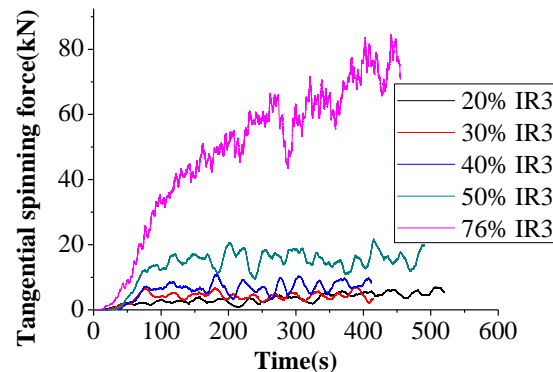
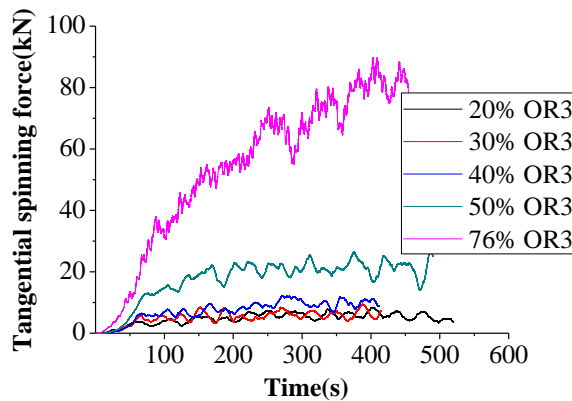


Figure 8 Tangential spinning force of OR3 Figure 9 Tangential spinning force of IR3

3.3. Effect of different roller forming angles on spinning force

Figure 10, Figure11 and Figure 12 respectively show the radial, axial and tangential spinning force under different forming angles of roller. In the stable stage, the average radical spinning force value is maximum when the forming angle of roller $\alpha_\rho=20^\circ$, as shown in Figure 10. The radical and tangential average spinning force value is minimum when the forming angle of roller $\alpha_\rho=25^\circ$, as shown in Figure 10 and Figure 12, respectively. The axial and tangential average spinning force value is maximum when the forming angle of roller $\alpha_\rho=30^\circ$, as shown in Figure 11 and Figure 12, respectively. The average axial spinning forces are similar when the forming angle of roller $\alpha_\rho=20^\circ$ and 25° .

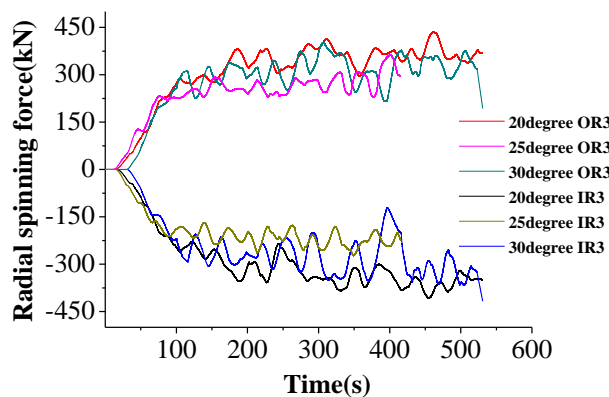


Figure 10 Radial spinning force of OR3 and IR3

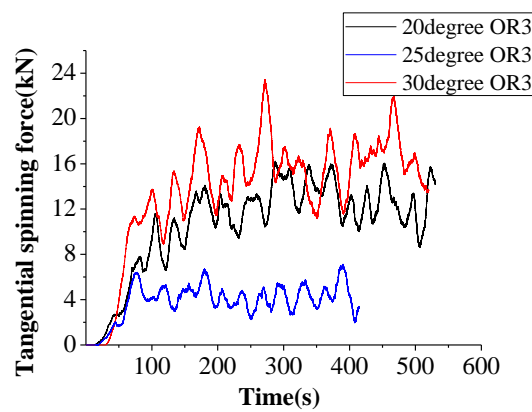
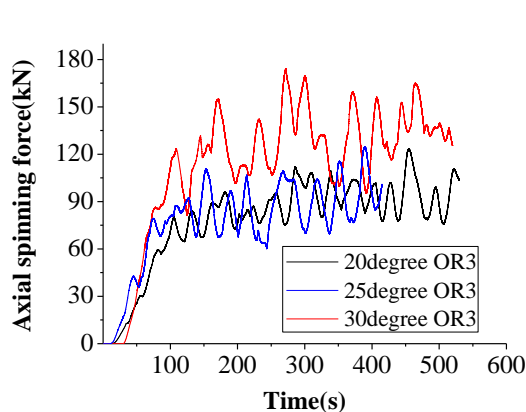


Figure 11 Axial spinning force of OR3 Figure12 Tangential spinning force of OR3

3.4. Effect of different feed rates on spinning force

Figure 13, Figure 14 and Figure 15 respectively show the radial, axial and tangential spinning force under different feed rates. With the increase of feed rate, the average radial, axial and tangential spinning force increase respectively. In addition, with the increase of feed rate, the difference of radial force between OR3 and IR3 increases gradually.

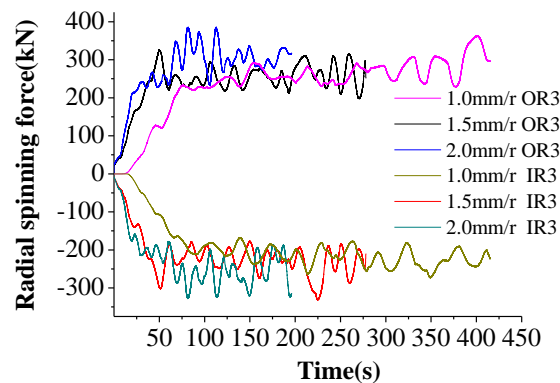


Figure 13 Radial spinning force of OR3 and IR3

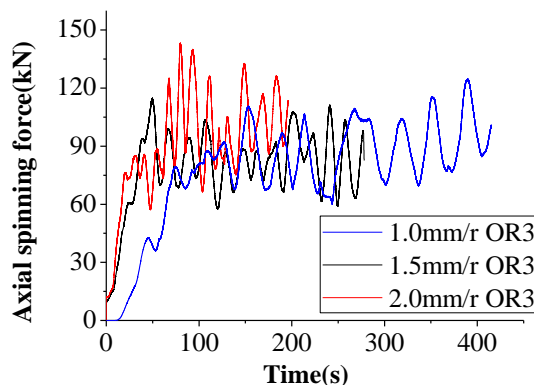


Figure 14 Axial spinning force of OR3

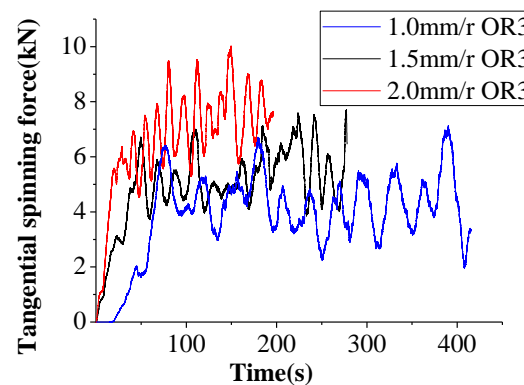


Figure 15 Tangential spinning force of OR3

4. Counter-roller spinning experiment

Based on the simulation results, the process parameters of counter-roller spinning experiment was determined as follows: thinning ratio $\Psi_t = 20\%$, feed rate $f = 1.0$ mm/r, forming angle of roller $\alpha_\theta = 25^\circ$. The process test of counter-roller spinning was carried out on the spinning machine equipped with 4 pairs of rollers, as shown in Figure 16. The radial spinning force was directly tested with a pressure tester, as shown in Figure 17.



Figure 16 Counter-roller spinning experiment

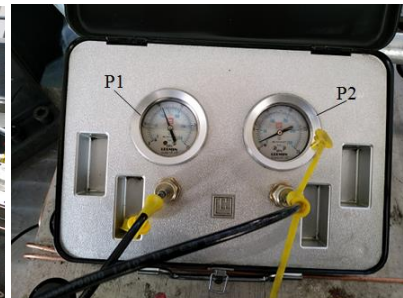


Figure 17 Force testing

Figure 18 shows the comparison of radial spinning force between simulation results and experiment results. It shows that the simulation results of radial spinning force conform well to the test results, the

relative average deviations between the test and simulation results are less than 12%. Figure19 shows the comparison of axial spinning force between simulation results and experiment results. The result shows that the relative average deviations between the test and simulation results are less than 10.5%. As can be seen from the figure, the simulated spinning force fluctuates greatly, while the test spinning force is very stable due to the metal grain size of the blank is much smaller than the mesh size in the simulation FEA model.

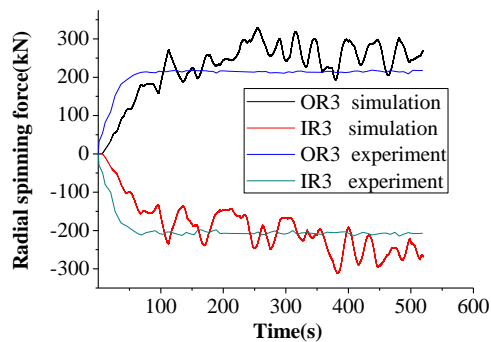


Figure18 Radial spinning force comparison

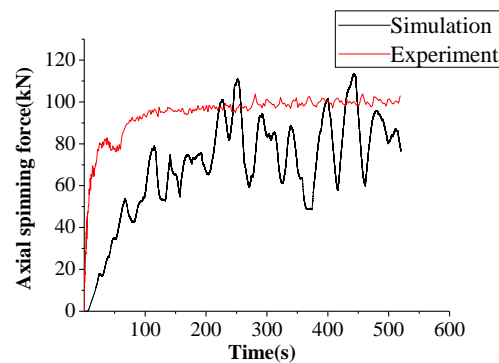


Figure19 Axial spinning force comparison

5. Conclusions

This paper studied the law of spinning force in the counter-roller spinning, and analyzed the influence of thinning ratio, feed rate and forming angle of roller on spinning force, and determined the reasonable process parameters, which provided technical guidance for the process test. The accuracy of simulating spinning force is verified by the spinning experiment.

1. The radial, axial and tangential spinning force respectively present a gradually increasing trend with the increase of the thinning ratio and feed rate.

2. In the stable stage, the average radical spinning force value is maximum when the forming angle of roller $\alpha_p=20^\circ$. The radical and tangential average spinning force value is minimum when the forming angle of roller $\alpha_p=25^\circ$. The axial and tangential average spinning force value is maximum when the forming angle of roller $\alpha_p=30^\circ$. The average axial spinning forces are similar when the forming angle of roller $\alpha_p=20^\circ$ and 25° .

3. The reasonable process parameters was determined by simulation as follows: thinning ratio $\Psi_t=20\%$, feed rate $f=1.0$ mm/r, forming angle of roller $\alpha_p=25^\circ$. The simulation results of radial spinning force conform well to the test results, the relative average deviations between the test and simulation results are less than 12%, and the relative average deviations of axial spinning force between the test and simulation results are less than 10.5%.

References

- [1] Xia QX, Xiao GF, Long H, Cheng XQ, Yang BJ (2014) A study of manufacturing tubes with nano/ultrafine grain structure by stagger spinning. *Mater Des* 59:516–523.
- [2] Xiao GF, Xia QX, Cheng XQ, Zhou YJ(2014) Research on the grain refinement method of cylindrical parts by power spinning. *Int J Adv Manuf Technol* 78:971-979.
- [3] Zhou XY(1993) Opposite roller spinning—A new process for manufacturing large tubes with high strength and precision. *Forging & Stamping Tchenology2*: 49-51(in Chinese).
- [4] Xia QX, Cheng XQ, Long H, Ruan F (2012) Finite element analysis and experimental investigation on deformation mechanism of non-axisymmetric tube spinning. *Int J Adv Manuf Technol* 59:263–272.
- [5] Xia QX, Cheng XQ, Hu Y, Ruan F (2006) Finite element simulation and experimental investigation on the forming forces of 3D nonaxisymmetrical tubes spinning. *Int J Mech Sci* 48(7):726–735.